Breaking of Rotational Symmetry during Decomposition of Elastically Anisotropic Alloys

O. Paris,[1] M. Fährmann,[2] and P. Fratzl[1]

[1]*Institut für Festkörperphysik der Universität Wien, Boltzmanngasse 5, A-1090 Wien, Austria*

[2]*Department of Materials Science and Engineering, Carnegie Mellon University, Pittsburgh, Pennsylvania 15213-3890*

(Received 23 May 1995)

The coarsening of a two-phase structure under the influence of interfacial energy alone is characterized by an isotropic domain morphology which evolves in a self-similar way with time. We have studied the breaking of rotational symmetry due to additional anisotropic elastic misfit interactions in the model alloy Ni-Al-Mo. Introducing a dimensionless parameter ρ as the ratio of elastic to interfacial energy, we show that, as long as $\rho < 1$, the spherically averaged structure function still has time-scaling properties. Under these conditions, the spatial anisotropy of the domains increases linearly with ρ and can be understood as a perturbation of the isotropic process at $\rho = 0$.

PACS numbers: 61.10.Lx, 64.70.Kb, 81.30.Mh

The domain patterns during coarsening of a two-phase structure [1] are usually found to evolve in a universal, self-similar way, as long as the reduction of interface energy remains the only driving force [2–6]. The structure function which characterizes the domain morphology and arrangement is then rotationally symmetric, and its evolution can be represented by a single typical length scale, e.g., the average domain size R [7–9]. In solid systems, such as metallic alloys, this universal behavior may be broken by the occurrence of long-range anisotropic interactions due to lattice strains [10–16]. The aim of the present work was to investigate this violation of universal scaling due to elastic anisotropy and to characterize the kinetics of this process. For this purpose, we have chosen the model system Ni-Al-Mo, which belongs to a class of alloys known as the nickel-based superalloys [17–22].

In these alloys, precipitate shapes are known to change from initially spherical to cuboidal- and plate-shaped morphologies [17–22]. The most striking effect is an almost periodic arrangement of the precipitates along the elastic soft directions, first found and discussed in terms of elastic interactions by Ardell, Nicholson, and Eshelby [17]. Since the elastic energy E_{el} scales with the volume of the domains and the interfacial energy E_S with their surface [12], the shape of the growing domains will typically change at sizes R, where E_{el} becomes comparable to E_S [12,14,21].

From these observations it becomes evident that the domain morphology is isotropic and its evolution self-similar when $E_{el} \approx 0$, but is highly anisotropic when $E_{el} > E_S$. The question arises whether in the intermediate regime, when

$$0 < \rho \equiv \frac{E_{el}}{E_S} < 1, \qquad (1)$$

the kinetics of domain coarsening may be described by a perturbation of the self-similar behavior at $E_{el} = 0$. In the present paper we show that, as long as the precipitates are not too large (that is $\rho < 1$), the spherically averaged structure function for Ni-Al-Mo alloys exhibits dynamical scaling behavior and that the scaling function is consistent with the universal curve found in systems without elastic misfit strains [8]. Also, the domain size R grows like $R \propto t^{1/3}$ [23] as a function of time t. The only deviation from scaling consists in the spatial anisotropy of the domains, which increases with time. Here we demonstrate for the first time that this anisotropy can be expressed in a very simple, universal way as a function of ρ for several Ni-Al-Mo alloys with different compositions, aging temperatures, and times. Only in the very late stages of coarsening, when $\rho > 1$, this picture breaks down and the time evolution cannot be represented as a function of R and ρ alone.

We have investigated the time evolution of the precipitate morphology in a series of six Ni-Al-Mo single crystals with different molybdenum content and, hence, different lattice constants a_m [21,22]. Since the elastic energy is proportional to the square of the lattice misfit $\delta = (a_p - a_m)/a_m$ (a_m and a_p are the unconstrained lattice constants of matrix and precipitates, respectively), alloys with different misfit values from -0.5% to $+0.65\%$ were studied in this way. One of the alloys had approximately zero misfit. After homogenizing and water quenching, the samples were isothermally aged at temperatures between 775 and 910 °C for different times. In this temperature range, the equilibrium volume fractions of precipitate phase are in the range between 10% and 20% for all six alloys [21,24].

The time evolution of the structure function was investigated by single crystal small angle x-ray scattering (SAXS) [25]. Figure 1 shows a typical SAXS spectrum $I(q, \Psi)$ in the $(1\bar{1}0)$ plane of reciprocal space with the main crystallographic directions indicated. q is the length of the scattering vector $\mathbf{q}$, and Ψ its angle measured with respect to the [001] direction. The scattering intensity—far from being isotropic—exhibits a strong maximum along [001], which is due to the preferred alignment of precipitates along this direction. First, the temporal evolution of the location of this interference peak

 0031-9007/95/75(19)/3458(4)$06.00

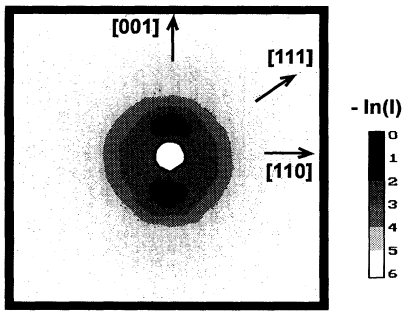

FIG. 1. The SAXS intensity is shown in a logarithmic pseudogrey scale versus scattering vector in the $(\bar{1}10)$ plane for the alloy with misfit $\delta = -0.5\%$ aged at 910 °C for 10 min. The scattering vector in the box ranges from -0.1 to 0.1 $Å^{-1}$ for the horizontal [110] direction and the vertical [001] direction. The main crystallographic directions are indicated by arrows.

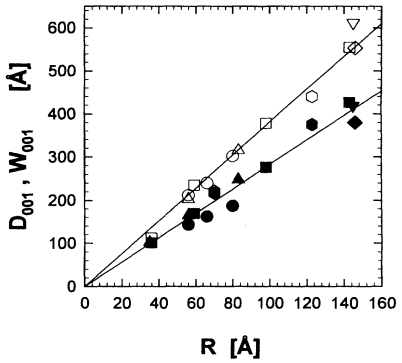

FIG. 2. The inverse location of the interference peak D_{001} (black symbols) and the inverse width of the structure function W_{001} (open symbols) are plotted versus the mean precipitate radius R. Different symbols correspond to different alloys and/or aging temperatures. The solid lines are linear fits to the data. The ratio D_{001}/W_{001} is approximately 0.75.

was obtained from the scattering vector $q_{\max}$ at the peak maximum by $D_{001} = 2\pi/q_{\max}$. Second, the full width at half maximum (FWHM) of the peak in radial direction was also determined and $W_{001} = 2\pi/\text{FWHM}$ calculated for all data sets. For the alloy with negligible misfit, the SAXS spectrum was found to be isotropic, and instead of a maximum in the [001] direction there was a ring-shaped intensity. Indeed, it is a well-known fact from decomposing alloys without elastic interactions that the intensity is isotropic and that a maximum of the same height appears along any crystallographic direction [1,8,9]. Third, to characterize the deviation from isotropy for the alloys with nonzero misfit we have determined the maximum intensity $I_m(\Psi) \equiv I(q_{\max}, \Psi)$ for all measurements. Finally, the mean precipitate radius R was evaluated as a radius of gyration using slices along the [111] direction [25], assuming that the precipitate shape is not too different from spherical. Indeed, for all the data presented here, the ratio ρ between elastic and interfacial energy does not much exceed unity where shape changes from sphere to cube usually start [14,21]. Most of the anisotropy in our data (see Fig. 1) is, in fact, due to an anisotropy of the arrangement and not so much of the shape of the precipitates.

Figure 2 shows a plot of D_{001} and W_{001} as a function of R. Both exhibit a linear dependence on R, which indicates a scaling behavior for these parameters. The ratio $\eta = D_{001}/W_{001} \approx 0.75$ is remarkably close to the values found for coarsening without elastic misfit interactions, where η varies from about 0.9 to about 0.75 for a volume fraction of precipitates between 10% and 20% [26]. Moreover, in agreement with previous work on the same alloy system [21], R was found to increase linearly with $t^{1/3}$. Hence, we conclude that all three parameters D_{001}, W_{001}, and R remain proportional to each other during coarsening and increase according to the Lifshitz-Slyozov-Wagner law [23]. If it were not for the anisotropy of the scattering spectra, one would conclude that the alloy system behaves exactly like a stress free system obeying scaling laws in time.

Nonetheless, there is a growing deviation from a self-similar evolution evident from our data, mostly due to particle alignment. This fact is reflected in the angular dependence of $I_m(\Psi)$, as shown for a few examples in Fig. 3. Generally, the SAXS intensity will deviate from its spherical average $\tilde{I}(q)$, but will reflect the cubic symmetry of the lattice. Consequently, we have tried to describe this deviation in terms of the cubic harmonics [27]

$$S_1(\mathbf{n}) = n_x^2 n_y^2 + n_x^2 n_z^2 + n_y^2 n_z^2, \tag{2}$$

$$S_2(\mathbf{n}) = n_x^2 n_y^2 n_z^2, \tag{3}$$

where $\mathbf{n} = \mathbf{q}/q$ denotes the unit vector in the direction of $\mathbf{q}$. (n_x, n_y, n_z) are the Cartesian coordinates of $\mathbf{n}$ with

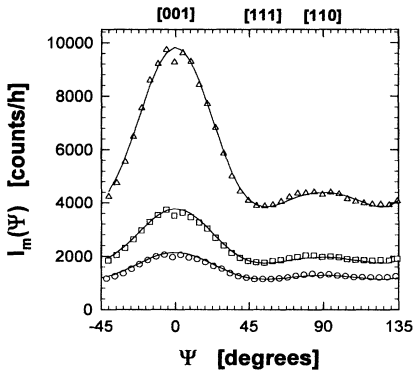

FIG. 3. Angular variation of the intensity $I_m(\Psi)$ at $q = q_{\max}$ with the angle Ψ in the $(11\bar{0})$ plane, for the alloy with misfit $\delta = -0.5\%$ aged at 780 °C for 32 min (circles), 100 min (squares), and 460 min (triangles). The main directions within this plane are indicated. The full lines are fits to the data using Eq. (4).

respect to the cubic crystal lattice. Fits of $I_m(\Psi)$ were performed using the function

$$I_m(\Psi) = \tilde{I}(q_{\max})[1 + \alpha P_1 + \beta P_2], \qquad (4)$$

where P_1 and P_2 are linear functions of S_1 and S_2, chosen so that their spherical average is zero, that is,

$$P_1 = 1 - 5S_1, \qquad P_2 = 1 - 105S_2, \qquad (5)$$

and where α and β are two constants. Figure 3 shows examples of fits with Eq. (4), where P_1 and P_2 were expressed as functions of the polar angle Ψ within the $(1\bar{1}0)$ plane.

The spatial anisotropy, as described by the constants α and β [see Eq. (4)], was found to increase with the domain size R as well as with the absolute value of the misfit δ. Generally, we expect the anisotropy to increase when the anisotropic part of the elastic energy E_{el}^a becomes larger with respect to the interfacial energy E_S. To estimate the ratio ρ of these energies [Eq. (1)], E_{el}^a was written in a rough approximation as $\frac{1}{2}|\Delta|\delta^2 V$ and E_S as $\sigma V/R$. Here $\Delta = (C_{11} - C_{12})/2 - C_{44}$ describes the elastic anisotropy (C_{11}, C_{12}, and C_{44} being the cubic elastic constants) [12], σ is the interface tension, V the total volume of the precipitates, and R their mean radius. Consequently, the ratio ρ can be expressed in terms of quantities accessible in experiments:

$$\rho = \frac{1}{2}|\Delta|\delta^2\frac{R}{\sigma}. \qquad (6)$$

A somewhat similar dimensionless parameter was already used by Voorhees and co-workers [14,20] to describe the shape evolution of a single misfitting precipitate in an infinite matrix. In their work, the shear modulus C_{44} instead of $|\Delta|$ was used to estimate the ratio between elastic and interfacial energy. It should be noted in this context that precipitate shape bifurcations are possible even in the elastic isotropic case ($\Delta = 0$), if the elastic moduli of matrix and precipitates are different [10,11,13]. However, since elastic anisotropy is the dominating contribution to the elastic energy in Ni-Al-Mo [28], the parameter $|\Delta|$ in Eq. (6) should reflect the right combination of elastic constants for this particular case. Nonetheless, even another combination of elastic constants would not alter the conclusions of the present paper, since Δ is not a function of time.

The coefficients α and β were fitted to the data using Eq. (4), and their dependence on the ratio ρ is shown in Fig. 4. In the presentation of the data, we took $\sigma = 20$ mJ/m^2 [17], $C_{11} = 232$ GPa, $C_{12} = 153$ GPa, and $C_{44} = 117$ GPa [29] for all alloys investigated. Most remarkably, both α and β exhibit a linear dependence on ρ for all our data as long as $\rho < 1$ ($\alpha \approx 2\rho$ and $\beta \approx \frac{1}{6}\rho$). This means that the evolution of the angular anisotropy can, in fact, be described with one parameter only, namely, the energy ratio ρ. Therefore the scattered

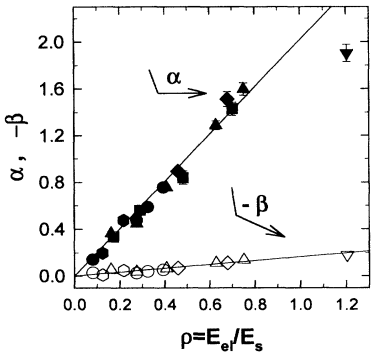

FIG. 4. The fit parameters α and $-\beta$ describing the spatial anisotropy [Eq. (4)] are plotted versus the ratio of elastic to interfacial energy ρ [Eq. (6)]. Different symbols correspond to different alloys and/or aging temperatures. The full lines correspond to $\alpha = 2.02\rho$ and $-\beta = 0.165\rho$.

intensity can be written for small ρ as

$$I(\mathbf{q}, t) \approx \tilde{I}(q, t)\,[1 + \rho(t)P(\mathbf{n})], \qquad (7)$$

where the spherically averaged intensity follows the usual scaling law

$$\tilde{I}(q, t) = R^3(t)\tilde{F}(q\,R(t)), \qquad (8)$$

F being the time independent scaling function [1,8,9]. The function P is also independent of time and given in terms of the cubic harmonics as

$$P \approx 2P_1 - \tfrac{1}{6}P_2. \qquad (9)$$

As long as $\rho < 1$, the structure function can be represented by Eq. (7), where the only time dependent parameters are R and ρ. However, when ρ exceeds unity, α begins to deviate from the linear behavior seen in Fig. 4. For even larger ρ, the [001] peak in $I_m(\Psi)$ (Fig. 3) becomes very narrow and cannot be represented by Eq. (4) anymore. Moreover, the ratio D_{001}/W_{001} ceases to be constant for $\rho > 1$ and increases due to a narrowing of the peak along the [001] direction. These effects are consistent with three-dimensional [15] and two-dimensional [30] computer simulation results . A dependence of the anisotropy on the volume fraction [19] might also be expected, but—as the volume fractions do not differ significantly for our alloys—this effect may not show up in our data.

In conclusion, the results reported here for Ni-Al-Mo alloys support the idea that, when $\rho < 1$, the effects of elastic anisotropy can be separated from an overall "interfacial energy driven" evolution of the microstructure. The mean structure parameters (e.g., precipitate size and distance) evolve according to the Lifshitz-Slyozov-Wagner law [23], and the spherically averaged structure function exhibits dynamical scaling [3,8,9]. The main effect induced by the elastic misfit interactions is the spatial anisotropy in the arrangement of the domains. Using a

perturbation approximation, the kinetics of the development of the anisotropy can be described by one parameter only, namely, the time dependent ratio ρ between elastic energy and interfacial energy. This simple picture was found to hold as long as ρ is smaller than unity.

This work was supported in part by the "Fonds zur Förderung wissenschaftlicher Forschung (FWF S5601)." Support from the "Deutsche Forschungsgemeinschaft (DFG)" and the "Alexander von Humboldt-Stiftung" is also gratefully acknowledged. We thank Professor William C. Johnson for helpful discussions and comments.

[1] J. D. Gunton, M. San Miguel, and P. S. Sahni, in *Phase Transitions and Critical Phenomena,* edited by C. Domb and J. L. Lebowitz (Academic Press, New York, 1983), Vol. 8; K. Binder, in *Materials Science and Technology,* edited by P. Haasen (VCH, Weinheim, New York, 1991), Vol. 5, Chap. 7.

[2] K. Binder and D. Stauffer, Phys. Rev. Lett. **33**, 1006 (1974).

[3] J. Marro, J. L. Lebowitz, and M. H. Kalos, Phys. Rev. Lett. **43**, 282 (1979).

[4] C. Roland and M. Grant, Phys. Rev. Lett. **60**, 2657 (1988).

[5] R. Toral, A. Chakrabarti, and J. D. Gunton, Phys. Rev. B **39**, 901 (1989).

[6] N. Akaiwa and P. W. Voorhees, Phys. Rev. E **49**, 3860 (1994).

[7] H. Furukawa, Adv. Phys. **34**, 703 (1985).

[8] P. Fratzl and J. L. Lebowitz, Acta Metall. **37**, 3245 (1989).

[9] P. Fratzl, J. L. Lebowitz, O. Penrose, and J. Amar, Phys. Rev. B **44**, 4794 (1991).

[10] J. D. Eshelby, Prog. Solid. Mech. **2**, 89 (1961).

[11] J. W. Cahn, Acta Metall. **10**, 179 (1962).

[12] A. G. Khachaturyan, *Theory of Structural Transformations in Solids* (Wiley, New York, 1983).

[13] A. Onuki and H. Nishimori, Phys. Rev. B **43**, 13 649 (1991).

[14] P. W. Voorhees, G. B. McFadden, and W. C. Johnson, Acta Metall. Mater. **40**, 2979 (1992).

[15] T. A. Abinandanan and W. C. Johnson, Acta Metall. Mater. **41**, 17 (1993).

[16] Y. Wang, L. Q. Chen, and A. G. Khachaturyan, Acta. Metall. Mater. **41**, 279 (1993).

[17] A. J. Ardell, R. B. Nicholson, and J. D. Eshelby, Acta Metall. **14**, 1295 (1966).

[18] T. Myazaki, M. Doi, and T. Kozakai, Solid State Phenom. **3**, 227 (1988).

[19] A. Maheshwari and A. J. Ardell, Phys. Rev. Lett. **70**, 2305 (1993).

[20] M. E. Thompson, C. S. Su, and P. W. Voorhees, Acta. Metall. Mater. **42**, 2107 (1994).

[21] M. Fährmann, P. Fratzl, O. Paris, E. Fährmann, and W. C. Johnson, Acta Metall. Mater. **43**, 1007 (1995).

[22] A. D. Sequeira, H. A. Calderon, G. Kostorz, and J. S. Pedersen, Acta. Metall. Mater. **43**, 3427 (1995); **43**, 3441 (1995).

[23] I. M. Lifshitz and V. V. Slyozov, J. Phys. Chem. Solids **19**, 35 (1961); C. Wagner, Z. Electrochem. **65**, 581 (1961).

[24] D. B. Miracle, V. Srinivasan, and H. A. Lipsitt, Metall. Trans. **A15**, 481 (1984).

[25] P. Fratzl, F. Langmayr, and O. Paris, J. Appl. Cryst. **26**, 820 (1993).

[26] P. Fratzl, J. Appl. Cryst. **24**, 593 (1991).

[27] A. G. Khachaturyan, S. V. Semenovskaya, and J. W. Morris Jr, Acta Metall. **36**, 1563 (1988).

[28] P. Fratzl and F. Langmayr, in *PTM 94, Solid-Solid Phase Transformations,* edited by W. C. Johnson, J. M. Howe, D. E. Laughlin, and W. A. Soffa (TMS, Warrendale, PA, 1994), p. 893.

[29] E. S. Fisher, Scr. Metall. **20**, 279 (1986).

[30] P. Fratzl and O. Penrose, Acta Metall. Mater. **43**, 2921 (1995); (to be published).

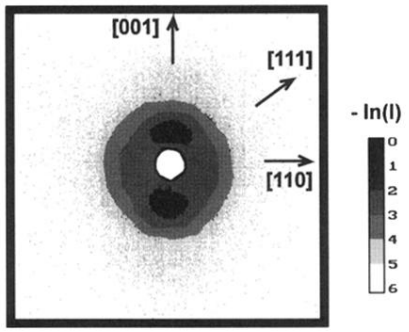

FIG. 1. The SAXS intensity is shown in a logarithmic pseudogrey scale versus scattering vector in the $(\bar{1}10)$ plane for the alloy with misfit $\delta = -0.5\%$ aged at 910 °C for 10 min. The scattering vector in the box ranges from -0.1 to 0.1 Å^{-1} for the horizontal [110] direction and the vertical [001] direction. The main crystallographic directions are indicated by arrows.